

Relationship Between Contrast Adaptation and Orientation Tuning in V1 and V2 of Cat Visual Cortex

N. A. Crowder, N.S.C. Price, M. A. Hietanen, B. Dreher, C.W.G. Clifford and M. R. Ibbotson

J Neurophysiol 95:271-283, 2006. First published Sep 28, 2005; doi:10.1152/jn.00871.2005

You might find this additional information useful...

This article cites 51 articles, 13 of which you can access free at:

<http://jn.physiology.org/cgi/content/full/95/1/271#BIBL>

Updated information and services including high-resolution figures, can be found at:

<http://jn.physiology.org/cgi/content/full/95/1/271>

Additional material and information about *Journal of Neurophysiology* can be found at:

<http://www.the-aps.org/publications/jn>

This information is current as of February 3, 2007 .

Relationship Between Contrast Adaptation and Orientation Tuning in V1 and V2 of Cat Visual Cortex

N. A. Crowder,¹ N.S.C. Price,¹ M. A. Hietanen,¹ B. Dreher,^{1,2} C.W.G. Clifford,³ and M. R. Ibbotson¹

¹Visual Sciences, Research School of Biological Sciences, Australian National University, Canberra; ²Department of Anatomy and Histology, School of Medical Sciences and Institute for Biomedical Research and ³Visual Perception Unit, School of Psychology, University of Sydney, Sydney, New South Wales, Australia

Submitted 18 August 2005; accepted in final form 25 September 2005

Crowder, N. A., N.S.C. Price, M. A. Hietanen, B. Dreher, C.W.G. Clifford, and M. R. Ibbotson. Relationship between contrast adaptation and orientation tuning in V1 and V2 of cat visual cortex. *J Neurophysiol* 95: 271–283, 2006. First published September 28, 2005; doi:10.1152/jn.00871.2005. Previous studies investigating the response properties of neurons in the primary visual cortex of cats and primates have shown that prolonged exposure to optimally oriented, high-contrast gratings leads to a reduction in responsiveness to subsequently presented test stimuli. We recorded from 119 neurons in cat V1 and V2 and found that in a high proportion of cells contrast adaptation also occurs for gratings oriented orthogonal to a neuron's preferred orientation, even though this stimulus did not elicit significant increases in spiking activity. Approximately 20% of neurons adapted equally to all orientations tested and a further 46% showed at least some adaptation to orthogonally oriented gratings, whereas 20% of neurons did not adapt to orthogonal gratings. The magnitude of contrast adaptation was positively correlated with adapting contrast, but was not related to the spiking activity of the cells. Highly direction selective neurons produced stronger adaptation to orthogonally oriented gratings than other neurons. Orientation-related adaptation was correlated with the rate of change of orientation tuning in consecutive cells along electrode penetrations that traveled parallel to the cortical layers. Nonoriented adaptation was most common in areas where orientation preference changed rapidly, whereas orientation-selective adaptation was most common in areas where orientation preference changed slowly. A minority of neurons did not show contrast adaptation (14%). No major differences were found between units in different cortical layers, V1 and V2, or between complex and simple cells. The relevance of these findings to the current understanding of adaptation within the context of orientation column architecture is discussed.

INTRODUCTION

Psychophysical studies of contrast adaptation have shown that prolonged exposure to high-contrast patterns leads to a decrease in the perceived contrast compared with nonadapted measures and a perceived fading of the adapting stimulus (Blakemore et al. 1973; Hammett et al. 1994; Snowden and Hammett 1996). Electrophysiological studies investigating contrast adaptation in the primary visual cortex of cats and primates have shown that a sigmoidal contrast response function is generated when a neuron's spike rate is plotted as a function of stimulus contrast. Prolonged exposure to optimally oriented, high-contrast gratings leads to reductions in responsiveness to subsequently presented test stimuli, which produce

rightward and/or downward shifts of a neuron's contrast response function (Bonds 1991; Carandini and Ferster 1997; Ohzawa et al. 1982, 1985; Sclar et al. 1989, 1990). Downward shifts are referred to as *response gain control* and rightward shifts as *contrast gain control* (for review see Ibbotson 2005).

The questions we address in this paper are: can nonoptimally oriented stimuli generate strong contrast adaptation and, if so, how common are such neurons in cat cortical areas V1 (area 17) and V2 (area 18; Payne and Peters 2002)? Furthermore, are these neurons found in selected regions of the cortical orientation maps? The question of adaptation to nonoptimal orientations is not new to the literature but a comprehensive study of response properties across all cortical layers based on a large cell sample has not been published. Moreover, this phenomenon has been investigated only in V1. Neurons in both V1 and V2 were included in this study to highlight any differences between these two cortical areas because they receive direct geniculate inputs originating mainly from X- and Y-cells, respectively (Burke et al. 1992; Dreher et al. 1992).

Below is a brief survey of available data on adaptation to nonoptimal grating orientations. Psychophysical studies have shown that contrast adaptation can be induced by gratings orthogonal to the test grating (Ross and Speed 1996; Snowden and Hammett 1992). In recordings from cat area V1, Vautin and Berkley (1977) showed that contrast adaptation was generated by gratings oriented orthogonally to the neuron's preferred orientation in two of 11 tested cells. Ohzawa et al. (1985) comment in their paper on contrast adaptation in cat V1 that they "have preliminary evidence that many cells may be adapted by presentation of stimuli of nonoptimal orientation." However, these data have not been made available in published form. In an abstract, Allison and Martin (1997) state that of 23 cat V1 neurons, the contrast response functions of only two cells were depressed after adaptation to orthogonal motion with a cross-oriented grating. Carandini et al. (1998) failed to show adaptation-related changes in spiking activity of V1 neurons after adaptation to orthogonal gratings in eight cells recorded intracellularly in cats and eight cells recorded extracellularly in monkeys. Some evidence of subthreshold activity changes was apparent from the cat data because the mean membrane potentials of the cells were slightly depolarized after adaptation to orthogonal gratings. The largest study of adaptation to orthogonal gratings was conducted by Sengpiel and Bonhoeffer (2002), who recorded from 80 neurons in layers 2 and 3 of cat

Address for reprint requests and other correspondence: M. R. Ibbotson, Visual Sciences, Research School of Biological Sciences, Australian National University, Canberra, ACT, Australia 2601 (E-mail: Michael.Ibbotson@anu.edu.au).

The costs of publication of this article were defrayed in part by the payment of page charges. The article must therefore be hereby marked "advertisement" in accordance with 18 U.S.C. Section 1734 solely to indicate this fact.

V1. Although this paper is the most comprehensive study to date, 58 of the cells were recorded while the cats were anesthetized with high halothane concentrations, which they suggest obscured adaptation to orthogonal gratings. From the remaining 22 cells, 12 showed adaptation to orthogonal gratings, suggesting for the first time that cross-orientation adaptation may be a common phenomenon.

A range of studies have looked at changes in orientation tuning, rather than contrast response functions, after adaptation at various nonoptimal orientations in area V1 in both cat and monkey (e.g., cat: Dragoi et al. 2000; monkey: Dragoi et al. 2002; Kohn and Movshon 2004; Müller et al. 1999). These studies provide additional evidence that adaptation to nonoptimal orientations can alter subsequent responses to optimally oriented gratings and alter the preferred orientation of cortical cells. In cats the postadaptation orientation tuning functions were least affected by adaptation to orthogonally oriented gratings and most to adaptation at orientations that differed by 0–60° from the preferred (Dragoi et al. 2000).

Here we record from 119 neurons to optimally oriented gratings moving in both preferred and antipreferred directions and to moving gratings oriented orthogonally. Recordings were made from all six layers of cat cortical areas V1 and V2, with an emphasis on cells in layer 4 (36% supragranular layers, 41% layer 4, and 23% infragranular layers). We show that around 20% of cortical neurons exhibit contrast gain control only to optimally oriented gratings (orientation-selective adaptation), whereas 20% show similar amounts of contrast adaptation to all adapting directions (nonoriented adaptation). The majority of cells show intermediate levels of orientation-related adaptation (46%) and some do not adapt to any orientation (14%). This is the first study to correlate contrast adaptation to non-optimally oriented gratings with the orientation, direction, and temporal frequency tuning properties of individual neurons. The results are discussed in the framework of intracortical circuits within the orientation maps of V1 and V2. Correlations between the rate of change in orientation tuning with electrode depth and the orientation tuning of contrast adaptation suggest that nonoriented adaptation may occur more often in pinwheel centers.

METHODS

Physiological preparation

Experimental procedures complied with the guidelines of the Australian National Health and Medical Research Council and were approved by the Animal Experimentation Ethics Committee of the Australian National University. Data were collected from six adult cats of either sex weighing between 2.8 and 4.2 kg. Animals were initially anesthetized with ketamine HCl (20 mg/kg, administered intramuscularly; Ilium, Smithfield, NSW, Australia) to allow the trachea and right cephalic vein to be cannulated. The head was held in a stereotaxic frame using ear bars, a mouth bar, and head bolt attached to the skull at the midline 3 cm anterior to interaural zero. A craniotomy was performed 0–8 mm posterior and 2–8 mm lateral to interaural zero to allow access to areas V1 and V2 with vertical electrode penetrations (using 1–1.5% halothane anesthesia). Neuro-muscular blockade was then induced with an intravenous injection of 50 mg of gallamine triethiodide (Flaxedil; Sigma, St. Louis, MO) in 2 ml of Hartmann's solution and maintained with continuous intravenous infusion of Flaxedil at a rate of 10 mg · kg⁻¹ · h⁻¹ in a 1:1:2 mixture of Hartmann's solution, 5% glucose, and 8% amino acid solution.

After initiation of paralysis, animals were ventilated with a pulmonary pump, and anesthesia was maintained with a mixture of gaseous halothane and a 2:1 ratio of N₂O and O₂. Expired CO₂ was monitored continuously and maintained at 3.5–4% by adjusting the breath rate or stroke volume of the pulmonary pump. The electrocardiogram (ECG) and electroencephalogram (EEG) were monitored continuously, and body temperature was maintained at 38°C with an electric heating blanket. Halothane was administered at 0.5% when recording from neurons and at 1–1.5% whenever surgical intervention was required (i.e., craniotomy, new electrode tracks, or injections). Increases in ECG or changes in the EEG suggesting a reduction in anesthesia were met with increases in the percentage of inhaled halothane. Such events occurred very rarely. Intramuscular injections of Clavulox (1 ml; Pfizer, West Ryde, NSW, Australia), dexamethasone sodium phosphate (1 ml; Ilium), and atropine (0.05 mg/kg; Apex Laboratories, Somersby NSW, Australia) were administered daily.

The corneas were protected with zero-power rigid gas-permeable contact lenses. Pupils were dilated and accommodation was paralyzed with 1% atropine sulfate eye drops (Sigma). The nictitating membranes were retracted with 0.01% phenylephrine HCl eye drops (Sanofi-Synthelabo, New York, NY). Corrective lenses and a streak retinoscope were used to focus the stimulus on the retina at a distance of 57 cm in front of the animal. Artificial pupils (3 mm diameter) were placed in front of the eyes to reduce spherical aberrations. The locations of the optic disc and area centralis of each eye were plotted twice daily by reverse ophthalmoscopy.

Extracellular recordings were made with lacquer-coated tungsten microelectrodes (FHC, Bowdoinham, ME) that were driven by a piezoelectric drive (Burleigh inchworm and 6000 controller, Burleigh Instruments, Rochester, NY). Extracellular signals from individual units were isolated, amplified, and filtered, then acquired with a CED1401 interface and Spike2 software (Cambridge Electronic Designs, Cambridge, UK) sampled at 40 kHz. A Schmitt trigger was also used to trigger TTL pulses, which were passed to Spike2 to allow on-line data analysis.

Stimuli and initial analysis

Locations of the dominant eye and receptive field (RF) of each neuron were initially determined using a hand-driven light bar. The nondominant eye was covered; quantitative testing was performed on the dominant eye with visual stimuli produced by a VSG Series 2/5 stimulus generator (Cambridge Research Systems, Cambridge, UK) and presented on a calibrated monitor (Eizo T662-T, 100-Hz refresh, 1,024 × 768 pixels) at a viewing distance of 57 cm. The location and size of the classical receptive field, as well as the preferred orientation/direction, spatial frequency (SF), and temporal frequency (TF), were determined by calculating on-line tuning functions for each stimulus parameter. Receptive field size was determined in two ways: 1) a circular patch of moving grating centered on the middle of the RF was expanded in size to find which diameter produced the optimal response; and 2) an annulus of moving grating was centered on the RF and the diameter of the empty center was decreased until spiking responses could just be elicited, thus indicating the edge of the excitatory RF. The size tuning function generated by the first measure indicated the diameter at which the response saturated, whereas the size tuning function generated by the second method indicated the outer boundary of the excitatory RF. Both measures usually agreed but, when they differed, the result from method 2 was used to set the stimulus size.

The stimulus for testing contrast adaptation was a sine-wave grating of optimal SF and TF presented in a circular aperture the size of the classical receptive field. The aperture had a diameter of 2–10° and

was surrounded by a gray of mean luminance (Lum; 50 cd/m²). Sine-wave contrast is defined as

$$\text{Michelson contrast} = \frac{(\text{Lum}_{\text{max}} - \text{Lum}_{\text{min}})}{(\text{Lum}_{\text{max}} + \text{Lum}_{\text{min}})}$$

Nonadapted contrast response functions were collected by presenting each contrast (0.04–1) in random order for 0.5-s tests (10 repetitions) interleaved with 4 s of mean luminance. Contrast response functions were measured for the neuron's preferred direction before and after adaptation regardless of the adaptor's motion direction. A 3-min recovery period was allowed between collecting the data for every contrast response function.

Adapted contrast response functions were collected in blocks, with the adaptor grating moving either in the neuron's preferred, antipreferred (preferred +180°), or orthogonal (preferred +90°) direction. Adaptation blocks consisted of 60 s of the adaptor followed by 0.5-s tests (aforementioned contrasts for 10 repetitions) interleaved with 4-s adaptation top-ups. Firing rates used to construct contrast response functions were calculated by taking the mean firing rate across repeats from 0.1 to 0.5 s after the test stimuli appeared. A full data set consisted of four contrast response functions: the nonadapted curve plus the three adaptation blocks. Often when a full data set was

collected, we would collect another full data set using a different adapting contrast. Typically, the adaptors had a contrast of 0.32 and the contrast that elicited approximately 50% maximum firing during the nonadapted control, which was estimated from a contrast response function produced on-line. Adapting contrasts of 0.16 and 1 were also frequently tested. Nonadapted contrast response functions were also repeatedly collected and compared to ensure the stability of extracellular isolations. Whenever the controls differed significantly between collecting full data sets, the data were excluded from further analysis. To test the generality of the adaptation effects seen in response to orthogonal and antipreferred gratings, 19 neurons were also tested with adaptors oriented at +45 and +135° to the preferred direction in addition to the usual preferred, antipreferred, and orthogonal adaptors.

Quantitative analysis

SIGMOIDAL FITS. In agreement with previous studies, the contrast response functions collected in the present study were suitably described by a sigmoid function (Fig. 1A; Sclar et al. 1989). Sigmoid curves were fitted using the equation

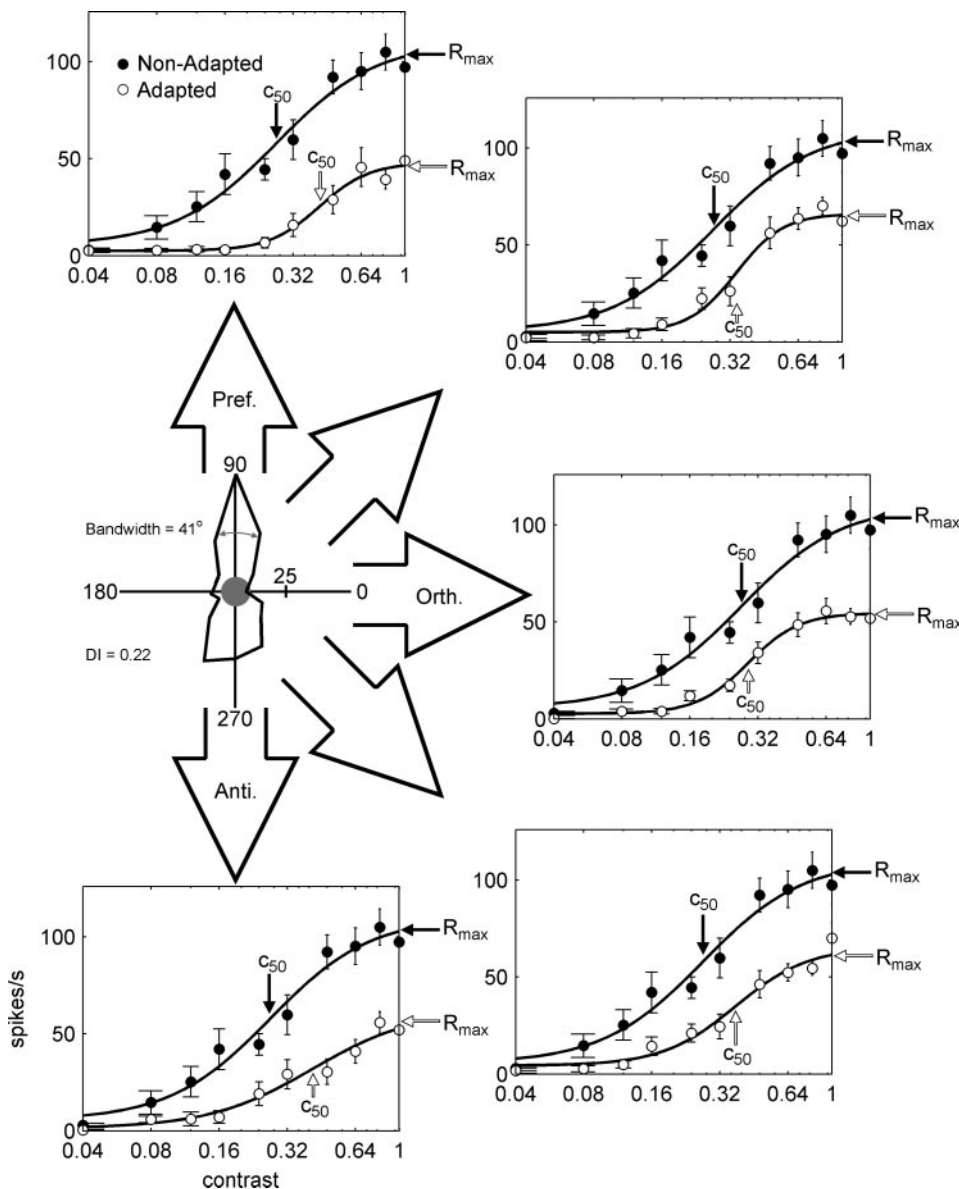


FIG. 1. Contrast adaptation in response to gratings moving in various directions. Polar plot shows the response amplitudes generated by motion in the indicated directions for a V2 neuron. Gray double-headed arrow shows the cell's orientation bandwidth. DI is the direction index. Large arrows indicate the directions of motion for adapting stimuli relative to the direction tuning of the cell. Neuron's nonadapted contrast response functions are shown with black dots. Circles show the adapted contrast response functions produced by gratings moving in the direction indicated. Lines represent best fits to a sigmoid function (see METHODS). Unadapted values of c_{50} and R_{max} are shown by black arrows, adapted values by white arrows. Pref., preferred; Anti., antipreferred; Orth., orthogonal.

$$R(c_i) = \frac{R_{\max} \times c_i^n}{c_i^n + c_{50}^n} + M$$

where $R(c_i)$ is the amplitude of the evoked response at contrast c_i , M is the spontaneous rate, n is the exponent that determines the steepness of the curve, R_{\max} is the maximum elevation in response above the spontaneous rate, and c_{50} is the contrast that generates a response elevation of half R_{\max} . Goodness of fit to the curve was measured with R^2 values, and across all fits this measure formed a highly skewed distribution with a median of 0.94. Rarely, contrast response functions did not show saturation at higher contrasts; in these cases the upper and lower R_{\max} bounds for the fit were set at $\pm 10\%$ of the maximum measured neuronal response above spontaneous. Furthermore, in rare cases where an adapted contrast response function became so flattened that the position of c_{50} became unreliable, c_{50} was assigned a value of 1 for that fit.

QUANTIFYING SHIFTS IN c_{50} AND R_{\max} . The following equations were used to quantify changes in c_{50} and R_{\max}

$$R_{\max \text{ shift}} = \frac{R_{\max \text{ adapted}} - R_{\max \text{ nonadapted}}}{R_{\max \text{ adapted}} + R_{\max \text{ nonadapted}}}$$

$$c_{50 \text{ shift}} = \frac{c_{50 \text{ adapted}} - c_{50 \text{ nonadapted}}}{c_{50 \text{ adapted}} + c_{50 \text{ nonadapted}}}$$

The difference over sum calculation normalizes the data such that a value of zero shows no change. Positive values of $c_{50 \text{ shift}}$ between 0 and 1 show varying degrees of adaptation (rightward shifts in c_{50}), whereas negative values indicate leftward shifts in c_{50} . Negative values of $R_{\max \text{ shift}}$ indicate response depression, whereas positive values indicate response enhancement. Previous studies suggest that adaptation would normally generate positive values of $c_{50 \text{ shift}}$ and negative values of $R_{\max \text{ shift}}$.

DIRECTION INDEX. Direction selectivity was measured quantitatively using the direction index (DI)

$$\text{Direction index} = \frac{[\text{spikes/s}_{\text{preferred}} - \text{spikes/s}_{\text{antipreferred}}]}{[\text{spikes/s}_{\text{preferred}} + \text{spikes/s}_{\text{antipreferred}}]}$$

Preferred motion refers to the direction that produced the largest spiking rate; antipreferred refers to the opposite direction. A cell was designated as direction selective only if the DI was >0.66 .

SIMPLE AND COMPLEX CELLS. Neurons were classified on-line as simple or complex based on qualitative tests performed with the light bar (Hubel and Wiesel 1962) and off-line by the relative modulation produced by a sine-wave grating. That is, we assigned simple and complex neurons using the ratio between modulated responses at the stimulus temporal frequency (F_1) and mean response (F_0) of the spiking responses to drifting sinusoidal gratings (Ibbotson et al. 2005; Skottun et al. 1991). Simple cells had F_1/F_0 ratios >1 , and complex cells had F_1/F_0 ratios <1 . F_1/F_0 ratios were calculated from the SF and TF tuning tests, which presented stimuli for 3 s. Simple and complex cells were classified using the optimum SF/TF (Skottun et al. 1991) and, because no cell had an optimum TF <1 Hz (Fig. 4C), F_1 values were calculated from at least three cycles.

Previous studies of contrast adaptation in the primary visual cortex of cats and primates calculated the response amplitude to a presented contrast using the F_1 amplitude for simple cells and F_0 amplitude for complex cells (Bonds 1991; Sclar et al. 1989). For our simple cells, the shapes but not the amplitudes of the contrast response functions were very similar using both the F_1 and F_0 amplitudes. However, the shifts in both c_{50} and R_{\max} were greater when using the F_0 measure, showing that in our experiments it was a more sensitive gauge of contrast adaptation. These observations agree with recent intracellular recording studies in cat V1, which showed that the F_1 component changes very little with contrast adaptation (Carandini and Ferster 1997; Sanchez-Vives et al. 2000a). Consequently, throughout this

paper, contrast response functions for simple cells, as for complex cells, are generated using F_0 amplitudes.

Histology

At the end of the recording session electrodes were moved back and forth 10 times using the piezoelectric drive (amplitude $50 \mu\text{m}$), always stopping at exactly the same depth. This was found to generate a buildup of cell damage produced by the tip of the electrode, which provided a good marker of the track depth without damaging the electrode by passing current through it. Then a different "lesion-electrode" was used to produce electrolytic lesions ($4 \mu\text{A}$, 5–10 s, electrode positive) at 2, 4, and 6 mm below the brain surface at a location displaced 3 mm medially from the recording site. This procedure generated clear lesions that could be correlated for depth with the recording tracks. By placing lesions at several known depths we were able to correct our track depths for the shrinkage commonly produced by fixatives.

Once depth markers were placed, animals were given a lethal dose of pentobarbitone sodium (120–180 mg depending on animal's weight) and immediately perfused with saline (0.9%) followed by 10% formal saline. Brains were extracted and cryoprotected in sucrose (30% in 0.1 M PB) for 2–10 days. Frozen sections ($45 \mu\text{m}$ thick in the coronal plane) from 0 through 8 mm posterior to interaural zero were collected. Sections were mounted onto gelatin chrome aluminum-coated slides and counterstained with thionin for Nissl substance. The tissue was then examined using light microscopy to confirm the locations of electrode tracks. Cell locations were reconstructed by correlating the electrode depths with the bottom of the track after taking account of brain shrinkage based on lesion markers.

RESULTS

Full data sets of the contrast adaptation protocol were obtained from 60 units in V1 and 59 units in V2. Receptive field centers were located 0 – 15° from the area centralis. We recorded from 43 complex and 17 simple units in V1 and 44 complex and 15 simple units in V2. Neurons in areas V1 and V2 showed similar trends for most measures of contrast adaptation, so results for both brain areas are discussed together.

Orientation tuning of contrast adaptation

Figure 1 shows contrast response functions for a representative complex neuron in V2. The polar plot on the left shows the response amplitudes following motion in the indicated directions with no prior adaptation. This cell was optimally responsive to horizontal gratings moving vertically upward. When the same grating was moved downward, strong excitation was also generated but with a significantly lower spike rate (t -test, $P < 0.015$). This neuron had a directional index of 0.22, so the cell was regarded as orientation selective but not direction selective (see METHODS). From the polar plot it is clear that vertically oriented gratings moving to the left or right did not produce responses that were significantly different from the mean spontaneous rate, which is indicated by the gray disc at the center of the polar plot. The orientation full-width half-maximum (FWHM) bandwidth is indicated by a double-headed arrow (41°).

The five graphs surrounding the polar plot show contrast response functions without prior adaptation (solid symbols) and after adaptation to gratings with contrasts of 0.32 moved in the directions indicated by the large arrows (open symbols). It is clear that for this cell contrast adaptation generated a

downward and leftward shift in the contrast response functions. Two parameters were extracted from the fitted curves (solid lines): R_{\max} , which is the maximum firing rate minus the spontaneous rate; and c_{50} , which is the contrast that generates an elevation in firing rate of half R_{\max} (see METHODS). For this neuron, adaptation is indicated quantitatively by the increases in c_{50} and decreases in R_{\max} . This cell is representative of neurons in which adaptation in all directions leads to strong adaptation regardless of the firing rate generated by the adapting stimulus. We refer to this as *nonoriented adaptation*.

Figure 2 shows four neurons that are representative of the spectrum of adaptation effects. The nonadapted contrast response function is represented by black dots, and responses after adaptation in the preferred, antipreferred, and orthogonal directions are shown as blue squares, green triangles, and red diamonds, respectively. Error bars represent SE values. The *inset* of Fig. 2 shows direction tuning polar plots for each neuron.

The cell in Fig. 2A is another example of a cell exhibiting nonoriented adaptation. All adapting orientations generate strong rightward shifts in the contrast response functions, even though the cell was tightly orientation selective and motion in the preferred direction produced more than twice the firing rate as motion in the antipreferred direction. Figure 2, B and C shows examples of two neurons at the opposite extreme of the orientation-related adaptation spectrum. Both of the neurons shown are orientation selective but not direction selective, i.e., they respond almost equally to horizontal gratings moved up or down but do not respond to horizontal motion of a vertically oriented grating. Adaptation to motion orthogonal to the pre-

ferred motion axis (i.e., left or right) does not change the contrast response function compared with the control condition. However, grating motion in either direction along the preferred motion axis (i.e., up or down) shifts the contrast response functions to the right and downward (Fig. 2, B and C). Clearly, in this type of cell, contrast adaptation is highly dependent on the orientation of the moving grating. We refer to this as *orientation-selective adaptation*. Figure 2D shows the adaptation characteristics of a neuron that falls in the middle of the orientation-related adaptation spectrum. It has a very narrow orientation tuning function and a DI of 0.49. Orthogonal, antipreferred, and preferred adaptation produce progressively greater rightward shifts in this cell's contrast response function.

For one V1 neuron and 18 V2 neurons we used adaptors oriented at $+45$ and $+135^\circ$ to the preferred direction in addition to the usual preferred, antipreferred, and orthogonal adaptors (e.g., Fig. 1). For all 19 neurons, the adaptation produced when these two additional stimuli were used was consistent with each cell's directional tuning characteristics and the adaptation produced by preferred, antipreferred, and orthogonal adaptors.

Population data

The results presented so far suggest a spectrum of adaptation effects. At one end of the spectrum are cells that exhibit orientation-specific adaptation (Fig. 2, B and C). At the opposite extreme are cells that show nonoriented adaptation (Figs. 1 and 2A), whereas most cells fall between these extremes (Fig.

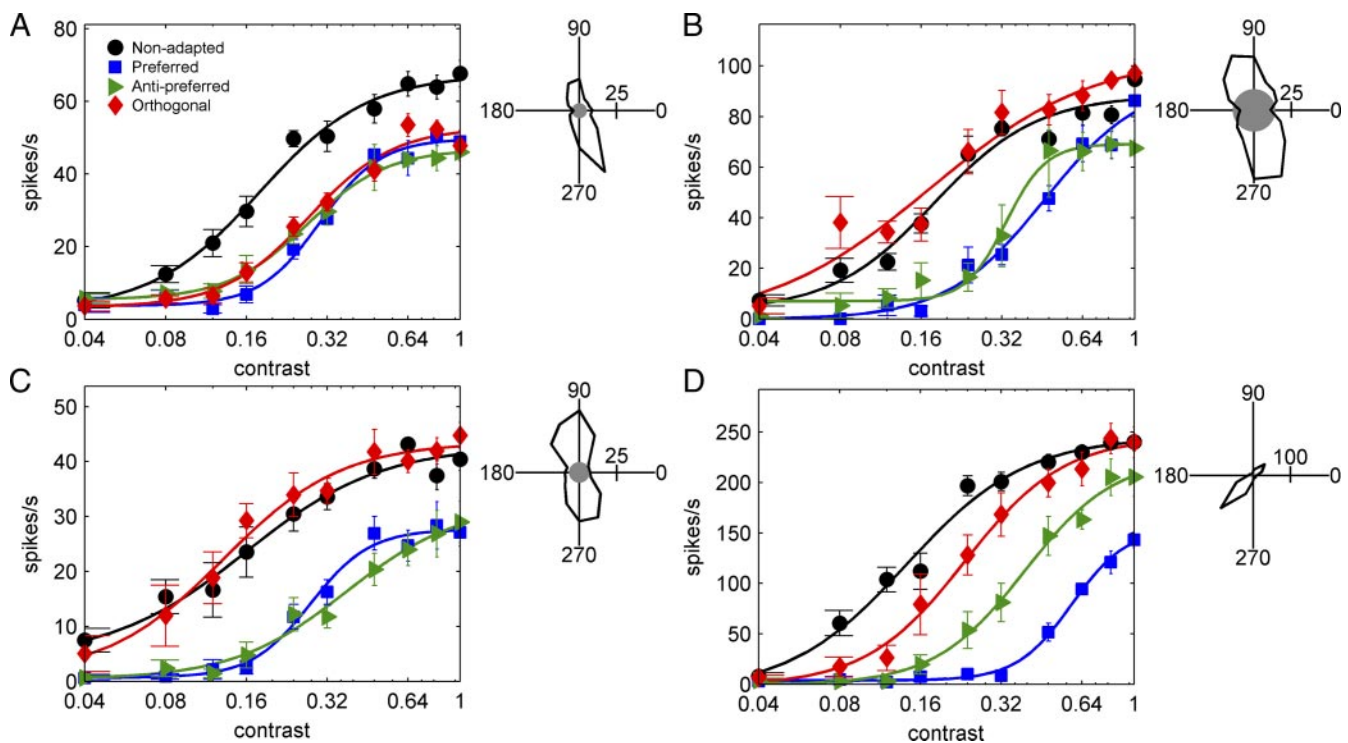


FIG. 2. Contrast response functions showing the spectrum of contrast adaptation effects from 4 V2 neurons: a cell exhibiting nonoriented adaptation (A); cells exhibiting orientation-selective adaptation (B, C); and a cell showing an intermediate type of adaptation in which all orientations generate some adaptation (D), but adaptation to preferred orientations is stronger. Contrast is on the abscissa, and mean response in spikes/s is on the ordinate. Nonadapted contrast response functions are shown as black dots and preferred, antipreferred, and orthogonal adaptation conditions are shown as blue squares, green triangles, and red diamonds, respectively. Error bars represent SE. *Inset*: orientation-tuning polar plots. Firing rate (spikes/s) is plotted as a function of stimulus direction in polar coordinates (gray area is the spontaneous rate).

2D). In addition to the cells that are part of the above spectrum, 17/119 neurons did not adapt to any stimulus orientation (nonadapting cells).

All population analysis used values of $c_{50 \text{ shift}}$ and $R_{\text{max shift}}$ to quantify changes in each neuron's contrast response functions (see METHODS). Both of these measures can have values between -1 and 1 . For $c_{50 \text{ shift}}$, 0 indicates no adaptation, whereas positive and negative values indicate rightward or leftward shifts of the contrast response functions, respectively. For $R_{\text{max shift}}$, 0 indicates no adaptation, whereas positive and negative values indicate increases or decreases of the maximum firing rate, respectively. Figure 3 shows histograms in which the total number of full data sets (226) collected at a range of adapting contrasts from 119 units is plotted against $c_{50 \text{ shift}}$ (left column) and $R_{\text{max shift}}$ (right column), after adaptation to optimally oriented gratings moved in the preferred (top row) and antipreferred directions (middle row), and to orthogonally oriented gratings moving at 90° to the preferred motion axis (bottom row). The means of the distributions of $c_{50 \text{ shift}}$ and $R_{\text{max shift}}$ are noted in each panel (Fig. 3). It is

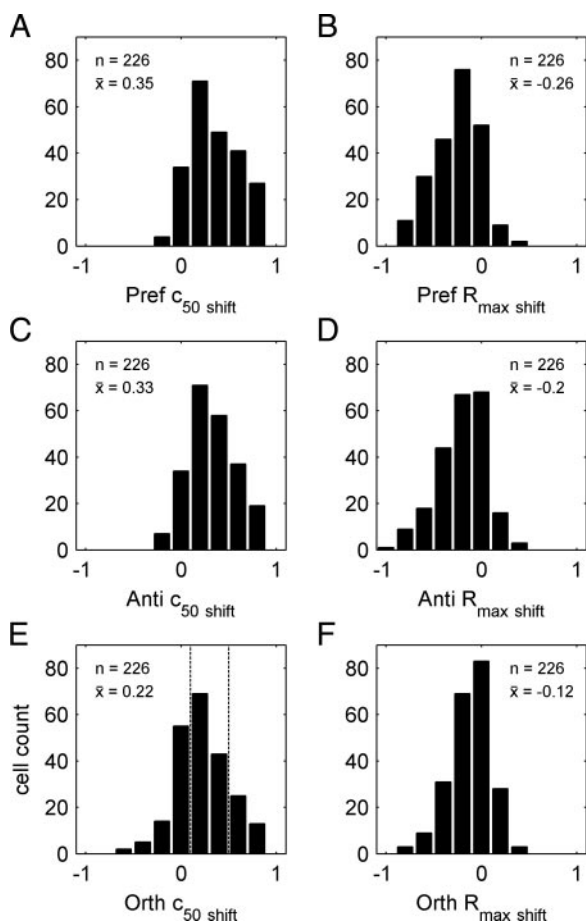


FIG. 3. Histograms showing the number of contrast adaptation tests (226) derived from 119 cells plotted against $c_{50 \text{ shift}}$ (left column) and $R_{\text{max shift}}$ (right column). Plots show these parameters after adaptation to optimally oriented gratings moved in the preferred direction (A, B), the antipreferred direction (C, D), and to orthogonally oriented gratings moved perpendicular to the preferred motion axis (E, F). Vertical lines in E show the boundaries that we have used to divide the cells into those that exhibit orientation-selective adaptation (<0.1), intermediate ($0.1-0.5$), and nonoriented adaptation categories (>0.5). Plots also contain data from 17 neurons that did not adapt to any grating orientation. Neurons in this latter category are massed close to $c_{50 \text{ shift}}$ and $R_{\text{max shift}}$ values of zero. Inset values show the means of the distributions.

evident that preferred direction motion produces a large rightward shift in c_{50} and a downward shift in R_{max} for most tests (Fig. 3, A and B). Furthermore, $c_{50 \text{ shift}}$ and $R_{\text{max shift}}$ show similar distributions after antipreferred direction motion (Fig. 3, C and D).

Adaptation to orthogonally oriented gratings produced the smallest mean values of $c_{50 \text{ shift}}$ and $R_{\text{max shift}}$ (Fig. 3, E and F), suggesting that orthogonal orientations generate less adaptation on average than preferred or antipreferred directions. Although the mean distribution shifts are smaller than with optimally oriented gratings, many individual cells show rightward shifts in c_{50} that are as large as those to optimally oriented gratings. These correspond to the cells that exhibit nonoriented adaptation. Also, note that after adaptation to orthogonally oriented gratings, several cells show a clear leftward shift in c_{50} (i.e., negative values of $c_{50 \text{ shift}}$ in Fig. 3E).

It is clear from inspection of the contrast response functions in Figs. 1 and 2 that it is the shift produced by orthogonal adaptation that distinguishes the different adaptation types. Therefore for the rest of this paper we use $c_{50 \text{ shift}}$ and $R_{\text{max shift}}$ from orthogonal adaptation to show the spectrum of orientation-related adaptation. Although no cells in our sample responded significantly to orthogonally oriented gratings, there was a clear spectrum of adaptation produced by this stimulus (Fig. 3E). For purely descriptive purposes we have set thresholds at values of $c_{50 \text{ shift}}$ of 0.1 and 0.5 (see dashed vertical lines in Fig. 3E). Neurons with values of $c_{50 \text{ shift}} < 0.1$ ($n = 23$) demonstrate orientation-selective adaptation, cells with values > 0.5 ($n = 24$) demonstrate nonoriented adaptation, and cells between these values have intermediate adaptation properties ($n = 55$). The 17 nonadapting neurons were excluded from the categories outlined above. Therefore from all 119 cells, 20% exhibit orientation-selective adaptation, 20% nonoriented adaptation, 46% intermediate adaptation, and 14% are nonadapting. For cells showing orientation-selective adaptation, 15 units were located in V1 and eight units were located in V2. For cells showing nonoriented adaptation, 14 units were located in V1 and 10 units were located in V2. For cells showing intermediate adaptation, 24 were located in V1 and 31 located in V2. Seven nonadapting cells were recorded in V1 and 10 were recorded in V2.

Relationship between adaptation and orientation selectivity

Figure 4 shows the relationship between each cell's orientation tuning and the amount of contrast adaptation induced by orthogonal gratings. The top histogram in Fig. 4A shows the distribution of orientation bandwidths (FWHM amplitude: see Fig. 1, polar plot). All of the cells have orientation bandwidths that fall between values of 23 and 148° , with a mean of 57° . Values of $c_{50 \text{ shift}}$ and $R_{\text{max shift}}$ from the orthogonal adaptation condition are plotted below the histogram as functions of the orientation bandwidths for all cells. Note that in most cells adaptation was studied with several adapting contrasts, so there are 226 points per scatterplot from 119 cells. Despite the relatively narrow orientation tuning bandwidths of most cells, bandwidth is poorly correlated with orthogonal $c_{50 \text{ shift}}$ ($R^2 = 0.02$) and orthogonal $R_{\text{max shift}}$ ($R^2 = 0.006$). Therefore it is not possible based solely on the orientation tuning of a given cell to predict its orientation-related adaptation properties. It is also evident, as shown in Fig. 3E, that a small group of cells

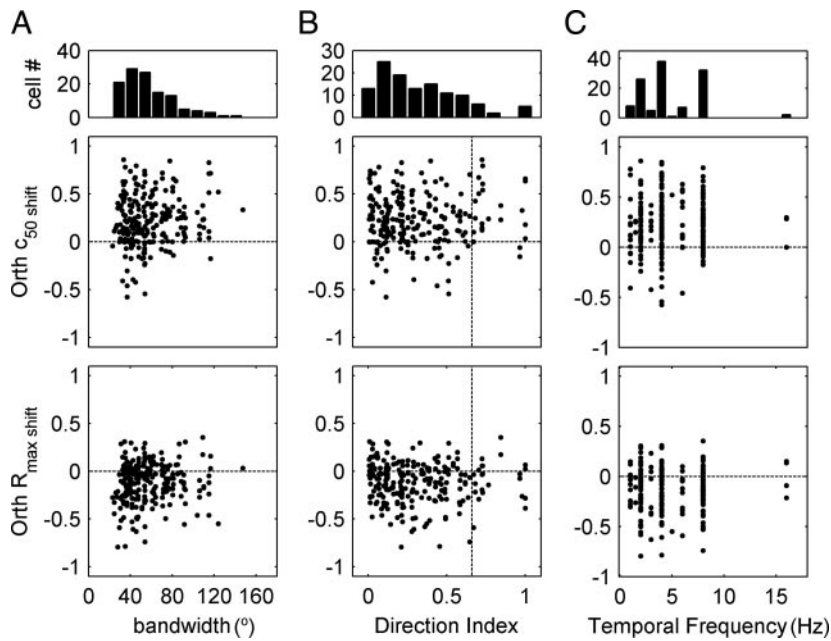


FIG. 4. Adaptation factors as functions of orientation bandwidth (left column: A), direction index (middle column: B), and temporal frequency (right column: C). Top row: cell number against each parameter. Middle and bottom rows: $c_{50 \text{ shift}}$ and $R_{\text{max shift}}$, respectively, after adaptation to orthogonally oriented gratings against bandwidth, DI, and TF. Vertical line in the 2nd column shows where the direction index is 0.66. We classified neurons with a DI >0.66 ($n = 14$) as highly direction selective.

consistently show leftward shifts in c_{50} after orthogonal adaptation (negative values of $c_{50 \text{ shift}}$, e.g., below the dotted line in the middle panel of Fig. 4A). This orthogonal facilitation may indicate that cross-orientation adaptation reduces the influence of inhibitory inputs in a small proportion of cells. For simplicity, these cells are included in the orientation-selective category.

Relationship with direction selectivity

We define a cell as direction selective if its direction index (DI) is >0.66 (see METHODS). The top panel in Fig. 4B shows the distribution of directional indices across the entire cell population. Of our cell population 105 are not direction selective and 14 are direction selective. Together they show a wide range of orientation-related adaptation effects. The mean values of $c_{50 \text{ shift}}$ for nondirectional and directional cells are $0.15 (\pm 0.26)$ and $0.38 (\pm 0.32)$, respectively. The mean values of $R_{\text{max shift}}$ for nondirectional and directional cells are $-0.08 (\pm 0.20)$ and $-0.08 (\pm 0.17)$, respectively. The values for nondirectional and directional cells are significantly different for $c_{50 \text{ shift}}$ (t -test, $P < 0.03$) but not for $R_{\text{max shift}}$ (t -test, $P > 0.98$). The findings indicate that on average highly directional cells produce larger rightward shifts in c_{50} after adaptation to orthogonally oriented gratings than cells with directional indexes <0.66 . The nonsignificant difference based on $R_{\text{max shift}}$ reflects a general finding that the maximum firing capacity of the cells is depressed by a similar amount regardless of the adaptation conditions (see Higher contrasts produce more adaptation, below, and Fig. 6).

We also correlated values of $c_{50 \text{ shift}}$ and $R_{\text{max shift}}$ obtained from adaptation to gratings moving in the antipreferred direction (Fig. 3, C and D) with DI. The mean values of $c_{50 \text{ shift}}$ for nondirectional and directional cells are 0.35 ± 0.28 (SD) and 0.42 ± 0.25 , respectively. The mean values of $R_{\text{max shift}}$ for nondirectional and directional cells are -0.2 ± 0.24 and -0.16 ± 0.26 , respectively. The values for nondirectional and directional cells are not significantly different for $c_{50 \text{ shift}}$ (t -

test, $P > 0.27$) or $R_{\text{max shift}}$ (t -test, $P > 0.42$). Thus in response to optimally oriented adapting stimuli moving in the antipreferred direction, neurons with high DI that responded very little to motion in the antipreferred direction showed similar adaptation to neurons with low DI that responded robustly to antipreferred motion. This result suggests that although contrast adaptation may be orientation selective for some neurons, it is not direction or firing rate dependent.

Relationship with temporal frequency

Figure 4C, top shows the distribution of optimum temporal frequencies for the 119 cells in this study. Note that the optimum TF was taken to be the value in our test grid that produced the highest spike rate rather than the peak of a fitted TF tuning curve, so the data points in Fig. 3C are aligned with specific TFs. The mean optimum TF for V1 cells was lower (3.6 ± 2.0 Hz) than that for V2 cells (6 ± 3.2 Hz). The values of $c_{50 \text{ shift}}$ and $R_{\text{max shift}}$ for the orthogonal adaptation condition are plotted against each cell's optimum TF in the middle and bottom panels, respectively. It is clear from these plots that the amount of adaptation to orthogonally oriented gratings was not related to the TF of the stimulus. The small number of cells that had very negative values of $c_{50 \text{ shift}}$ after orthogonal adaptation tended to have lower preferred TFs (>6 Hz). The finding that TF does not affect orthogonal adaptation agrees with the finding that adaptation effects were similar in V1 and V2 based on histological cell location (see Factors not linked to orientation-related adaptation).

Orientation-tuning of adaptation does not change with adapting contrast

For 83% of neurons, several full adaptation protocols were repeated with more than one adapting contrast. For neurons that were tested with more than one adapting contrast, 85% showed the same type of orientation-related adaptation across all adapting contrasts. As an example, Fig. 5 shows a neuron that was tested with three adapting contrasts (0.32, 0.66, and 1;

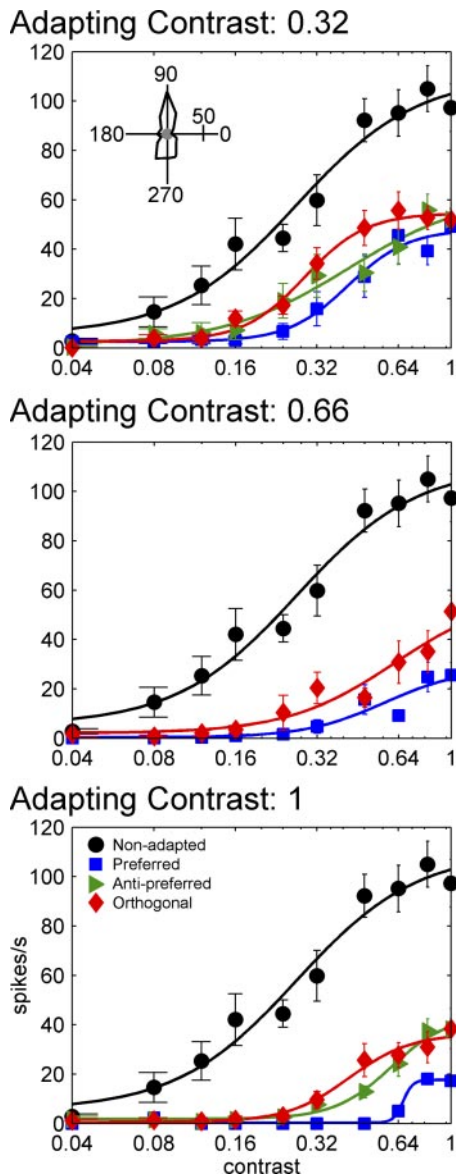


FIG. 5. Contrast adaptation in response to adaptors of various contrasts. Contrast response functions from a single V2 neuron when the adapting stimuli were gratings with contrasts of 0.32 (top), 0.66 (middle), and 1.0 (bottom). Inset: orientation tuning.

same cell as Fig. 1). Despite the large differences in the contrast of the adapting stimuli, the contrast response functions arising from various adapting directions maintain their position relative to each other. In those units that had different properties at different adapting contrasts, there was a tendency to shift from orientation-selective adaptation to nonoriented adaptation as contrast increased.

Higher contrasts produce more adaptation

Our data indicate that R_{\max} shows no systematic changes as contrast increases, regardless of the adapting orientation. That is, across the population all contrasts cause similar reductions in R_{\max} . However, rightward shifts in c_{50} become larger as the adapting contrast increases, supporting previous observations that contrast gain control is a fundamental property of cortical adaptation (e.g., Ohzawa et al. 1985). Although this was shown

previously, the data presented here constitute the first time that contrast gain-related changes have been shown for adaptation to both preferred and orthogonal orientations. To show the population data in a meaningful way, we have normalized the stimulus contrast into a value that indicates relative adapting strength (A_s). This measure takes account of the different values of c_{50} in the unadapted condition between cells

$$A_s = (c_{\text{adaptor}} - c_{50 \text{ nonadapted}}) / (c_{\text{adaptor}} + c_{50 \text{ nonadapted}})$$

where A_s is the strength of the adaptor relative to the nonadapted c_{50} , and c_{adaptor} is the contrast of the adapting grating. This equation normalizes the adapting strength of the stimulus such that zero represents an adapting contrast equal to the nonadapted c_{50} . Thus positive values of A_s represent adaptation at contrasts above the nonadapted c_{50} and negative values of A_s represent contrasts below c_{50} . Therefore adapting at positive A_s values generally produced large rightward shifts in c_{50} .

Figure 6, A–C shows A_s plotted against $R_{\max \text{ shift}}$ for the three adapting directions. Although R_{\max} values generally decreased after adaptation, the amplitude of the decrease was not related to the adapting contrast. The low R^2 values for fitted linear regression lines for the relationship between A_s and $R_{\max \text{ shift}}$ are shown on the plots. Note that a common adapting contrast was the estimate of the neuron's nonadapted c_{50}

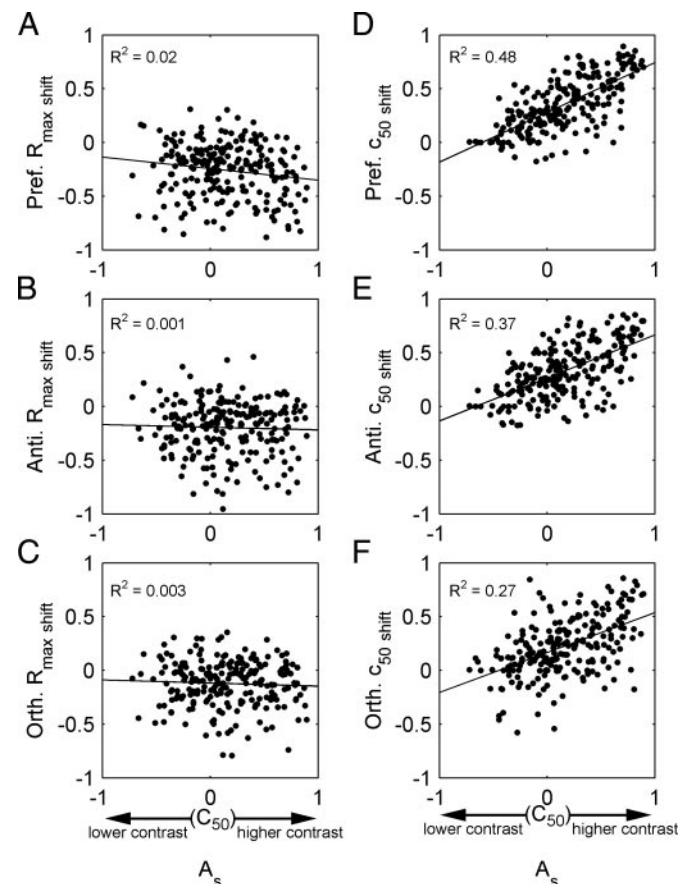


FIG. 6. Effect of adapting contrast on the R_{\max} and c_{50} of contrast response functions. A–C: relative strength of the adapting contrast (A_s) plotted against preferred, antipreferred, and orthogonal $R_{\max \text{ shift}}$ population data. Solid lines indicate the regression line, and the coefficient of determination (R^2) is noted in the top left of each scatterplot. D–F: A_s values plotted against preferred, antipreferred, and orthogonal $c_{50 \text{ shift}}$ population data.

calculated on-line. As such, one might expect a large proportion of dots on the scatterplots to align at an A_s of zero. However, because the on-line estimation of c_{50} was only approximate, these A_s values scatter around zero. Figure 6, *D–F* shows A_s plotted against $c_{50 \text{ shift}}$ for the three adapting directions. There was a strong relationship between adapting contrast and $c_{50 \text{ shift}}$ for all the adapting directions of motion. Relatively high contrasts (positive A_s values) produced increases in c_{50} , whereas relatively low contrasts (negative A_s values) produced lower $c_{50 \text{ shift}}$ values. The relationship between adapting contrast and $c_{50 \text{ shift}}$ was linear, as revealed by good fits to linear regression lines (Fig. 6, *D–F*; R^2 values, *inset*). In summary, adaptation usually reduces maximum firing rates regardless of contrast, but changes in c_{50} are related linearly to adapting contrast for all adapting orientations/directions.

Correlation of orientation-related adaptation and orientation columns

We made a total of 10 vertical electrode penetrations in six cats. All tracks were made adjacent to the marginal sulcus (MS) with three tracks penetrating only area V1 and seven rostral tracks penetrating first area V1 then V2 (for an example of the latter track positions and orientations see Fig. 1 in Hubel and Wiesel 1965). The V1/V2 border was noted during recording when a marked shift in receptive field position occurred and was confirmed histologically using the increased thickness of layer 3 as a measure (Payne 1990). We recorded from 43 units located in the supragranular layers (1–3), 49 units in layer 4, and 27 units located in the infragranular layers (5–6).

The trajectory of our electrode penetrations was such that each track passed through a number of orientation columns (Bonhoeffer and Grinvald 1991; Hubel and Wiesel 1974). The average distance between recorded units was 176 μm (SD 236). Along tracks made parallel to the cortical surface, cells of the same adaptation type (e.g., orientation-selective adaptation vs. nonoriented adaptation) tended to cluster together. Of the units recorded in this study, 54/119 (45%) were grouped in clusters of two or more cells that were classified as the same contrast adaptation type (based on the divisions shown in Fig. 3*E*). There was no statistical difference in the distance between units for those cells grouped in clusters and cells that were not surrounded by similarly classified cells ($P > 0.85$, Student's *t*-test). Orientation pinwheels are spaced approximately every 1 mm on the cortical surface (Bonhoeffer and Grinvald 1991; Das and Gilbert 1999; Maldonado et al. 1997). Given the average distance between recorded units relative to the distance between pinwheel centers, the observed proportion of clustering is consistent with the scale of the columnar orientation maps of the primary visual cortex, suggesting that this organization may relate to the adaptation effects described herein.

To quantify a relationship between orientation-related adaptation types and the orientation columns of the cortex we performed the following calculations. We identified cells as belonging to one of four adaptation categories: 1) orientation-selective adaptation; 2) intermediate; 3) nonoriented adaptation; and 4) nonadapting (as shown in Fig. 3*E*). We then selected cells that were isolated consecutively (no more than 400 μm apart) that were in the same adaptation category. The average distance between cells in this subset of 46 neurons was

131 μm (SD 111). The maximum interunit distance of 400 μm was chosen because it is approximately half the diameter of an orientation hypercolumn. For all these regions of the tracks we calculated the mean difference in orientation tuning between consecutive recordings from the same adaptation type. We also calculated the mean difference in depth between those recordings. A ratio of those two values was then calculated for the different cell categories. We did not isolate any nonadapting cells in consecutive recordings, so they are not discussed further. We were able to identify 11, 21, and 14 units in the orientation-selective adaptation, intermediate, and nonoriented adaptation categories, respectively. Figure 7 plots the mean orientation/depth ratios from those cells.

The mean ratio for cells exhibiting orientation-selective adaptation was 0.07, whereas the values for intermediate and nonoriented adaptation were 0.31 and 0.34. The differences between the first and the last two values were significant (*t*-test, <0.01). The very low value for orientation-selective adaptation indicates that the mean change in orientation was very small relative to the depth change between recordings (e.g., 7° orientation change per 100 μm). This suggests that these neurons were recorded in iso-orientation regions of the cortical sheet, where orientation changes little with distance. Conversely, cells exhibiting nonoriented adaptation showed relatively large changes in orientation relative to electrode depth (e.g., 34° orientation change per 100 μm). This result implies that the cells exhibiting nonoriented adaptation were located close to pinwheel centers in the cortical sheet where orientation changes rapidly with distance. The intermediate adaptation category produced orientation/depth ratios intermediate between the other two categories but was not significantly different from the nonoriented category. This result implies that this broad class of cells was recorded in the intermediate zones between pinwheel centers and iso-orientation zones.

Factors not linked to orientation-related adaptation

ABSOLUTE SPIKING RATE. The response of an unadapted neuron to unity contrast was used to approximate the maximum firing

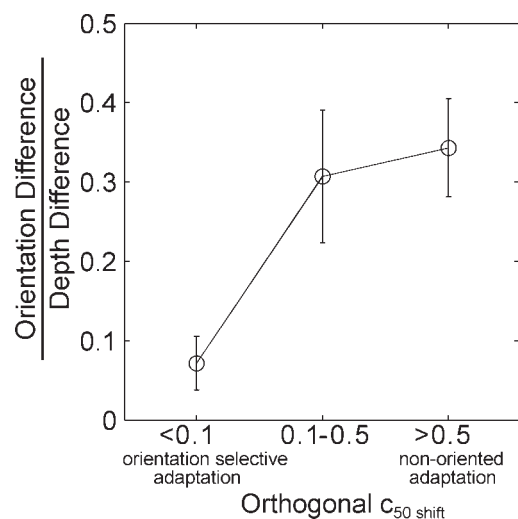


FIG. 7. Ratio of the mean change in preferred orientation and the mean change in depth for cells classified as having orientation-selective adaptation ($n = 11$), intermediate adaptation properties ($n = 21$), and nonoriented adaptation ($n = 14$). Errors are SE.

rate that could be elicited using our stimuli. The average maximum firing rate for all neurons that showed clear adaptation to preferred orientations was 88 (SD 66) spikes/s. Of the 17/119 neurons that did not adapt, the mean firing rate at maximum contrast was 52 (SD 38) spikes/s. The difference in firing rate between adapting and nonadapting neurons was significant ($P < 0.0004$, Student's *t*-test). Therefore neurons not showing contrast adaptation to our protocol have significantly lower maximum firing rates than those of neurons that do adapt. However, between the cell types that do adapt, there was no significant difference in maximum firing.

Given the relationship between firing rate and stimulus orientation/direction (*insets*: Figs. 1, 2, and 5), we needed to determine whether the spiking rate in the adapted state correlated with the amplitude of adaptation. For each cell, the mean spiking rate during the top-up adaptation periods (normalized to the maximum rate across directions) was used as a measure of spiking rate in the adapted state. For each measure of firing rate produced by a particular adapting stimulus, $R_{\max \text{ shift}}$ and $c_{50 \text{ shift}}$ were used to determine the amount of adaptation. For each cell we compared all combinations of contrast and direction. There was a poor correlation between firing rate in the adapted state and the amount of adaptation. For $R_{\max \text{ shift}}$ the relationship between adapted spiking rate and adaptation had a slope < 0.001 with an $R^2 < 0.001$, whereas for $c_{50 \text{ shift}}$ the slope was 0.21, with an $R^2 = 0.001$. Thus the firing rate of a neuron when it is in an adapted state does not predict the amplitude of adaptation, regardless of adapting orientation.

OTHER CELL PROPERTIES. We correlated the values of $c_{50 \text{ shift}}$ derived from the orthogonal adaptation protocols with three further cell attributes: 1) simple versus complex cells; 2) cells located in V1 versus V2 (see *Population data*, above); and 3) the locations within specific cortical layers (see *Correlation of orientation-related adaptation and orientation columns*, above). We do not present these correlations in any formal way because there were no significant differences in the relative proportions of any of the orientation-related adaptation properties when comparing these factors.

DISCUSSION

We have shown that about 20% of neurons in cat cortical areas V1 and V2 adapt only to orientations that generate clear spiking responses (orientation-selective adaptation). Although this result implies that the firing rates of the neurons may dictate the amount of adaptation, an analysis comparing adaptation measures at various adapting contrasts and orientations that generate differing spiking rates reveals that stimulus orientation rather than absolute spiking rate is the determining factor. Conversely, about 20% of the neurons can be classified as cells in which the amount of adaptation is equal regardless of the orientation of the adapting stimulus (nonoriented adaptation). The majority of adapting cells fall between these two extreme adaptation conditions (46%). We stress that the categories listed above do not form separate distributions but are simply a descriptive means of dividing a continuum into quantifiable groupings. Approximately 14% of the cells in our population did not adapt to any stimulus orientation and, interestingly, they had the lowest mean firing rates at maximum contrast. It is possible that our monocular stimulus

regime did not optimally stimulate these cells. This implies that in these cases the stimulus was not selective enough to generate adaptation.

Several authors have shown that orthogonally oriented gratings can generate contrast adaptation, although the reported cell populations are small (e.g., Allison and Martin 1997; Ohzawa et al. 1985; Sengpiel and Bonhoeffer 2002; Vautin and Berkley 1977). Herein we present data from 119 neurons and conclusively show that a relatively large proportion of neurons in V1 and V2 show adaptation to orthogonal stimuli. Moreover, we show that a spectrum of orientation-related adaptation effects exists.

Influence of anesthesia

Sengpiel and Bonhoeffer (2002) recorded from 80 cells in layers 2 and 3 of cat V1. They found very few cells that adapted to orthogonal gratings when using 0.7% inhaled halothane as the anesthetic. However, in one cell where the percentage of halothane was lowered to 0.4%, and in cells recorded using 1.1% isoflurane, more orthogonal adaptation was observed. The amount of orthogonal adaptation was likely related to the dosage of anesthesia rather than the type of anesthetic. In fact, Villeneuve and Casanova (2003) suggest that isoflurane is inferior to halothane for single-cell recordings because it has stronger depressive effects at equipotent concentrations. Our usage of 0.5% halothane probably generated similar effects to the 0.4% of Sengpiel and Bonhoeffer (2002) because both of these relatively low concentrations revealed the adaptation.

Measures of adaptation

Contrast gain control refers to lateral shifts of the contrast response function that center the c_{50} on prevailing contrasts, whereas response gain control refers to a vertical compression of the contrast response function that causes a general decrease in firing (for review see Ibbotson 2005). Our data support and extend the well-known observation that contrast gain control is the prevalent effect of contrast adaptation in the striate cortex (Bonds 1991; Carandini and Ferster 1997; Ohzawa et al. 1982, 1985; Sclar et al. 1989). Although many of our neurons showed at least some decrease in maximum firing rates to all adapting orientations (reduced response gain), this decrease was similar for most contrasts. Conversely, shifts in c_{50} to all adapting orientations were linearly related to the adapting contrast. Whereas single-unit data usually show some evidence of covariance between contrast gain and response gain, the population data reveal that only changes in c_{50} depend on the relative strength of the adapting stimulus. Therefore from population coding and behavioral perspectives contrast gain should be the dominant adaptive effect. Where our data extend previous knowledge is in showing that contrast gain control is also the dominant adaptive effect for adaptation to optimally oriented gratings moving in the antipreferred direction and to orthogonally oriented gratings, thus supporting mechanisms in which a unified gain control mechanism works across the cortical surface in areas V1 and V2 (Bonds 1991).

Sengpiel and Bonhoeffer (2002) recorded from 22 cells in layers 2 and 3 of cat V1 under isoflurane anesthesia. From this population, they identified 12 (55%) that adapted to orthogonal

gratings. This is similar to the proportion of cells in our population (66%) that showed at least some adaptation to orthogonal orientations (nonoriented and intermediate groups combined). Despite the similarities in these percentages, their test procedure and analysis methods create some problems in interpreting their data. First they collect responses at only three test contrasts for each adapting contrast (e.g., adapt at 0.07 and test at 0.035, 0.07, and 0.14). Second, the highest adapting contrast for which a three-point contrast response function was collected was 0.28 and the highest contrast presented was 0.56. Therefore their data spanned only half the available range of contrasts and tended to capture only the rising section of neurons' contrast response functions. Third, they assess adaptation with a statistical method that fits their data to two models: nonadapting and contrast gain control. If their adaptation index (AI) is >1 it favors contrast gain control and if it is <1 it favors nonadaptation. Even for optimally oriented gratings, the majority of their AI values are <1 , revealing very few neurons that showed clear contrast gain control.

A limitation of their model-driven analysis method is that it does not take account of changes in the slope and maximum amplitude of the contrast response functions caused by changes in response gain (e.g., their Fig. 2B). As discussed above, we found that response and contrast gain covaried in virtually all cells. Therefore in an adapting cell where response and contrast gain occur together, neither of the models in the analysis reported by Sengpiel and Bonhoeffer (2002) would be entirely appropriate. If cells had been tested with a wider range of contrasts it is possible that the influence of response gain control would have been revealed. We are confident that our methods of data collection (including anesthetic state) and analysis provide sensitive measures of adaptation that take account of both response and contrast gain control.

Generating different types of orientation-related adaptation

Bonds (1991) noted that network-driven contrast adaptation seems advantageous over the independent adaptation of single neurons because the visual system must function as a whole, and uniform gain control across the network would preserve the neuronal activity gradient representing the visual scene independent of adaptation state. Recent intracellular studies have shown that contrast adaptation produces hyperpolarization of the membrane potential, which may partially arise from intrinsic membrane mechanisms (Carandini and Ferster 1997; Sanchez-Vives et al. 2000a,b). However, Sanchez-Vives et al. (2000a) caution that intrinsic membrane mechanisms must work together with synaptic mechanisms to produce contrast adaptation because sinusoidal current injection produced less hyperpolarization than visual stimulation and adaptation can be produced without action potentials (this was also observed in the present study).

A likely site for the synaptic mechanisms involved in contrast adaptation is in local intracortical networks, where a range of synaptic interactions have been reported (e.g., Monier et al. 2003). Single-unit and optical imaging studies have shown that orientation selectivity is organized in a columnar fashion across primary visual cortex with iso-orientation regions that converge at pinwheel centers (Bonhoeffer and Grinvald 1991; Hubel and Wiesel 1974; Maldonado et al. 1997). Furthermore, individual cortical neurons receive inputs from local networks

encompassing 500–800 μm of the surrounding cortex independent of orientation preference (Das and Gilbert 1999). Therefore the orientation information carried by a cell's local network would depend on its location within the orientation map. Neurons located in pinwheel centers would receive inputs with a broad range of orientation preferences, whereas neurons located in iso-orientation regions would receive inputs with similar orientation preferences (Das and Gilbert 1999; Dragoi et al. 2001; Monier et al. 2003).

The continuum of adaptation effects seen in the present study is reminiscent of the continuum of effects seen in the adaptation-dependent orientation plasticity of area V1. Dragoi et al. (2001) showed that neurons located in iso-orientation regions, with neighbors that prefer similar orientations, showed minimal changes in orientation tuning after adaptation to non-optimal orientations. Neurons located at pinwheel centers, with neighbors that prefer a broad range of orientations, showed a large degree of orientation plasticity. The local network inputs that influence orientation plasticity may be linked to contrast adaptation, as studied here.

Sengpiel and Bonhoeffer (2002) proposed that if a neuron was located in a pinwheel center and received adaptive inputs from neighboring cells with various orientation preferences, nonoriented adaptation might be expected. Conversely, if a neuron was located in an iso-orientation region it might be expected to exhibit orientation-selective contrast adaptation. However, when recording selectively from pinwheel centers and iso-orientation domains by guiding their electrodes using optical imaging of the cortical surface, they found no significant differences based on their AI measure (see *Measures of adaptation*, above).

In our study there appears to be a correlation between the rate of change of orientation and the type of adaptation. In areas with the greatest rate of change in orientation we more frequently isolated cells with nonoriented adaptation properties. Conversely, in areas with little orientation change we identified cells with orientation-selective adaptation. This finding fits with the theory proposed by Sengpiel and Bonhoeffer, but not with their data. When the effect of anesthesia is taken into account, their reliable data on correlating orientation maps to adaptation are based on 22 cells and our data are based on 46 cells. Because both studies rely on a small data set and show conflicting findings, future studies using appropriate anesthesia, intrinsic optical imaging techniques, and analysis using full contrast response functions will constitute the only method for clarifying the issue.

An alternative theory to explain nonoriented adaptation is that such cells inherit their adaptive properties from precortical neurons with nonoriented center-surround receptive fields [retina: Baccus and Meister 2002; Chander and Chichilnisky 2001; dorsal lateral geniculate nucleus (LGNd): Solomon et al. 2004]. Although many studies in cat LGNd did not uncover contrast adaptation (Bonds 1991; Movshon and Lennie 1979; Ohzawa et al., 1985), the high-contrast adaptation protocol used by Sanchez-Vives et al. (2000a) did reveal modest LGNd contrast adaptation (also see Shou et al. 1996). However, it is unlikely that this modest adaptation could fully account for the large shifts in contrast response functions observed in the present study, and adaptation in the LGNd cannot explain the orientation-selective adaptation seen in many cells. We therefore consider a cortical network model of adaptation properties

to be the most likely mechanism leading to the spectrum of orientation-related adaptation properties that we have observed.

Orientation-related contrast adaptation across brain areas

Although both areas V1 and V2 constitute the primary visual cortex in the cat, their direct input from the LGNd is quite different (for review see Dreher 1986; Dreher et al. 1980; Payne and Peters 2002). Area V1 receives its principal dorsal thalamic input from X-type cells in the LGNd, whereas area V2 receives its LGNd input mainly from Y-type cells and has no X-type input (for reviews see Burke et al. 1992; Dreher et al. 1980, 1992; Stone and Dreher 1973). Despite receiving different input from the LGNd, cells in areas V1/V2 show a similar spectrum of orientation-related adaptation effects. These results correlate well with the finding that nearly half of X-type and Y-type LGNd neurons exhibit some degree of contrast adaptation (Shou et al. 1996). Furthermore, the strong interconnectivity between these two areas could also account for their similar adaptation properties (Freund et al. 1985a,b; Hollander and Vanegas 1977; Humphrey et al. 1985a,b; Price 1985; Price et al. 1994).

Contrast adaptation to orthogonal gratings and cross-orientation suppression

Neurons in V1 tend to produce temporal frequency tuning functions that peak at lower values (<4 Hz) than cells in V2 (2–8 Hz) (Movshon et al. 1977). These findings are similar to ours, which found mean optimum TF tuning of 3.6 and 6.0 Hz for V1 and V2, respectively. Allison et al. (2001) found that cross-orientation suppression of V1 cells was strongest when the mask grating had a TF of about twice that of the neuron's preferred TF. They suggest that cross-orientation suppression in V1 might arise from oriented V2 inputs. In the current study, we showed that the magnitude of contrast adaptation produced by orthogonal gratings did not depend on the adapting grating's TF and was similar for neurons in V1 and V2. This result suggests that cross-orientation suppression and contrast adaptation are produced by different mechanisms, with the possible exception of the small number of neurons that showed orthogonal facilitation after contrast adaptation. Monier et al. (2003) reported that the diversity in the way inhibitory and excitatory inputs are combined in V1 could result from nonhomogeneous lateral intracortical connections. The majority of evidence suggests that contrast adaptation mainly affects excitatory inputs (e.g., Carandini and Ferster 1997). We found that orthogonal facilitation, which may result from adaptation of cross-orientation inhibition, was extremely rare. This result agrees with the finding that neither γ -aminobutyric acid nor bicuculline administration affects contrast adaptation in V1 (DeBruyn and Bonds 1986; McLean and Palmer 1996; Vidyasagar 1990).

ACKNOWLEDGMENTS

Thanks go to Professor Jonathan Victor for useful discussions on the topic and to S. Durant and S. Wilson for help during recording sessions. Exceptional veterinary care was provided by K. Debono, K. Wall, and the late R. Cameron.

GRANTS

This work was supported by grants to M. Ibbotson and C. Clifford from the National Health and Medical Research Council, to M. Ibbotson from the

Institutes of Advanced Studies, and to N. Crowder from the National Science and Engineering Research Council of Canada. B. Dreher was supported while on sabbatical by a grant from the Centre for Visual Sciences at the Australian National University.

REFERENCES

- Allison JD and Martin KAC. Contrast adaptation produced by null direction and cross orientation stimulation of neurons in cat visual cortex. *Soc Neurosci Abstr* 23: 454, 1997.
- Allison JD, Smith KR, and Bonds AB. Temporal-frequency tuning of cross-orientation suppression in the cat striate cortex. *Vis Neurosci* 18: 941–948, 2001.
- Baccus SA and Meister M. Fast and slow contrast adaptation in retinal circuitry. *Neuron* 36: 909–919, 2002.
- Blakemore C, Muncey JP, and Ridley RM. Stimulus specificity in the human visual system. *Vision Res* 13: 1915–1931, 1973.
- Bonds AB. Temporal dynamics of contrast gain in single cells of the cat striate cortex. *Vis Neurosci* 6: 239–255, 1991.
- Bonhoeffer T and Grinvald A. Iso-orientation domains in cat visual cortex are arranged in pinwheel-like patterns. *Nature* 353: 429–431, 1991.
- Burke W, Dreher B, Michalski A, Cleland BG, and Rowe MH. Effects of selective pressure block of Y-type optic nerve fibers on the receptive-field properties of neurons in the striate cortex of the cat. *Vis Neurosci* 9: 47–64, 1992.
- Carandini M and Ferster D. A tonic hyperpolarization underlying contrast adaptation in cat visual cortex. *Science* 276: 949–952, 1997.
- Carandini M, Movshon JA, and Ferster D. Pattern adaptation and cross-orientation interactions in the primary visual cortex. *Neuropharmacology* 37: 501–511, 1998.
- Chander D and Chichilnisky EJ. Adaptation to temporal contrast in primate and salamander retina. *J Neurosci* 21: 9904–9916, 2001.
- Das A and Gilbert CD. Topography of contextual modulations mediated by short-range interactions in primary visual cortex. *Nature* 399: 655–661, 1999.
- DeBruyn EJ and Bonds AB. Contrast adaptation in cat visual cortex is not mediated by GABA. *Brain Res* 383: 339–342, 1986.
- Dragoi V, Rivadulla C, and Sur M. Foci of orientation plasticity in visual cortex. *Nature* 411: 80–86, 2001.
- Dragoi V, Sharma J, Miller EK, and Sur M. Dynamics of neuronal sensitivity in visual cortex and local feature discrimination. *Nat Neurosci* 5: 883–891, 2002.
- Dragoi V, Sharma J, and Sur M. Adaptation-induced plasticity of orientation tuning in adult visual cortex. *Neuron* 28: 287–298, 2000.
- Dreher B. Thalamocortical and corticocortical interconnections in the cat visual system: relations to the mechanisms of information processing. In: *Visual Neuroscience*, edited by Pettigrew JD, Sanderson KJ, and Levick WR. Cambridge, UK: Cambridge Univ. Press, 1986.
- Dreher B, Leventhal AG, and Hale PT. Geniculate input to cat visual cortex: a comparison of area 19 with areas 17 and 18. *J Neurophysiol* 44: 804–826, 1980.
- Dreher B, Michalski A, Cleland BG, and Burke W. Effects of selective pressure block of Y-type optic nerve fibers on the receptive-field properties of neurons in area 18 of the visual cortex of the cat. *Vis Neurosci* 9: 65–78, 1992.
- Freund TF, Martin KA, Somogyi P, and Whitteridge D. Innervation of cat visual areas 17 and 18 by physiologically identified X- and Y-type thalamic afferents. II. Identification of postsynaptic targets by GABA immunocytochemistry and Golgi impregnation. *J Comp Neurol* 242: 275–291, 1985a.
- Freund TF, Martin KA, and Whitteridge D. Innervation of cat visual areas 17 and 18 by physiologically identified X- and Y-type thalamic afferents. I. Arborization patterns and quantitative distribution of postsynaptic elements. *J Comp Neurol* 242: 263–274, 1985b.
- Hammett ST, Snowden RJ, and Smith AT. Perceived contrast as a function of adaptation duration. *Vision Res* 34: 31–40, 1994.
- Hollander H and Vanegas H. The projection from the lateral geniculate nucleus onto the visual cortex in the cat. A quantitative study with horseradish-peroxidase. *J Comp Neurol* 173: 519–536, 1977.
- Hubel DH and Wiesel TN. Receptive fields, binocular interaction and functional architecture in the cat's visual cortex. *J Physiol* 160: 106–154, 1962.
- Hubel DH and Wiesel TN. Receptive fields and functional architecture in two nonstriate visual areas (18 and 19) of the cat. *J Neurophysiol* 28: 229–289, 1965.
- Hubel DH and Wiesel TN. Sequence regularity and geometry of orientation columns in the monkey striate cortex. *J Comp Neurol* 158: 267–293, 1974.

- Humphrey AL, Sur M, Uhlrich DJ, and Sherman SM.** Projection patterns of individual X- and Y-cell axons from the lateral geniculate nucleus to cortical area 17 in the cat. *J Comp Neurol* 233: 159–189, 1985a.
- Humphrey AL, Sur M, Uhlrich DJ, and Sherman SM.** Termination patterns of individual X- and Y-cell axons in the visual cortex of the cat: projections to area 18, to the 17/18 border region, and to both areas 17 and 18. *J Comp Neurol* 233: 190–212, 1985b.
- Ibbotson MR.** Physiological mechanisms of adaptation in the visual system. In: *Fitting the Mind to the World: Adaptation and Aftereffects in High-Level Vision*, edited by Clifford C and Rhodes G. Oxford, UK: Oxford Univ. Press, 2005, p. 17–45.
- Ibbotson MR, Price NSC, and Crowder NA.** On the division of cortical cells into simple and complex types: a comparative viewpoint. *J Neurophysiol* 93: 3699–3702, 2005.
- Kohn A and Movshon JA.** Adaptation changes the direction tuning of macaque MT neurons. *Nat Neurosci* 7: 764–772, 2004.
- Maldonado PE, Godecke I, Gray CM, and Bonhoeffer T.** Orientation selectivity in pinwheel centers in cat striate cortex. *Science* 276: 1551–1555, 1997.
- McLean J and Palmer LA.** Contrast adaptation and excitatory amino acid receptors in cat striate cortex. *Vis Neurosci* 13: 1069–1087, 1996.
- Monier C, Chavane F, Baudot P, Graham LJ, and Fregnac Y.** Orientation and direction selectivity of synaptic inputs in visual cortical neurons: a diversity of combinations produces spike tuning. *Neuron* 37: 663–680, 2003.
- Movshon JA and Lennie P.** Pattern-selective adaptation in visual cortical neurons. *Nature* 278: 850–852, 1979.
- Movshon JA, Thompson ID, and Tolhurst DJ.** Spatial and temporal contrast sensitivity of neurones in areas 17 and 18 of the cat visual cortex. *J Physiol* 283: 101–120, 1977.
- Müller JR, Metha AB, Krauskopf J, and Lennie P.** Rapid adaptation in visual cortex to the structure of images. *Science* 285: 1405–1408, 1999.
- Ohzawa I, Sclar G, and Freeman RD.** Contrast gain control in the cat visual cortex. *Nature* 298: 266–268, 1982.
- Ohzawa I, Sclar G, and Freeman RD.** Contrast gain control in the cat's visual system. *J Neurophysiol* 54: 651–667, 1985.
- Payne BR.** Representation of the ipsilateral visual field in the transition zone between areas 17 and 18 of the cat's cerebral cortex. *Vis Neurosci* 4: 445–474, 1990.
- Payne BR and Peters A.** *The Cat Primary Visual Cortex*. London: Academic Press, 2002.
- Price DJ.** Patterns of cytochrome oxidase activity in areas 17, 18 and 19 of the visual cortex of cats and kittens. *Exp Brain Res* 58: 125–133, 1985.
- Price DJ, Ferrer JM, Blakemore C, and Kato N.** Functional organization of corticocortical projections from area 17 to area 18 in the cat's visual cortex. *J Neurosci* 14: 2732–2746, 1994.
- Ross J and Speed HD.** Perceived contrast following adaptation to gratings of different orientations. *Vision Res* 36: 1811–1818, 1996.
- Sanchez-Vives MV, Nowak LG, and McCormick DA.** Membrane mechanisms underlying contrast adaptation in cat area 17 in vivo. *J Neurosci* 20: 4267–4285, 2000a.
- Sanchez-Vives MV, Nowak LG, and McCormick DA.** Cellular mechanisms of long-lasting adaptation in visual cortical neurons in vitro. *J Neurosci* 20: 4286–4299, 2000b.
- Sengpiel F and Bonhoeffer T.** Orientation specificity of contrast adaptation in visual cortical pinwheel centres and iso-orientation domains. *Eur J Neurosci* 15: 876–886, 2002.
- Sclar G, Lennie P, and DePriest DD.** Contrast adaptation in striate cortex of macaque. *Vision Res* 29: 747–755, 1989.
- Shou T, Li X, Zhou Y, and Hu B.** Adaptation of visually evoked responses of relay cells in the dorsal lateral geniculate nucleus of the cat following prolonged exposure to drifting gratings. *Vis Neurosci* 13: 605–613, 1996.
- Skottun BC, De Valois RL, Grosf DH, Movshon JA, Albrecht DG, and Bonds AB.** Classifying simple and complex cells on the basis of response modulation. *Vision Res* 31: 1079–1086, 1991.
- Snowden RJ and Hammett ST.** Subtractive and divisive adaptation in the human visual system. *Nature* 355: 248–250, 1992.
- Snowden RJ and Hammett ST.** Spatial frequency adaptation: threshold elevation and perceived contrast. *Vision Res* 36: 1797–1809, 1996.
- Solomon SG, Peirce JW, Dhruv NT, and Lennie P.** Profound contrast adaptation early in the visual pathway. *Neuron* 42: 155–162, 2004.
- Stone J and Dreher B.** Projection of X- and Y-cells of the cat's lateral geniculate nucleus to areas 17 and 18 of visual cortex. *J Neurophysiol* 36: 551–567, 1973.
- Vautin RG and Berkley MA.** Responses of single cells in cat visual cortex to prolonged stimulus movement: neural correlates of visual aftereffects. *J Neurophysiol* 40: 1051–1065, 1977.
- Vidyasagar TR.** Pattern adaptation in cat visual cortex is a co-operative phenomenon. *Neuroscience* 36: 175–179, 1990.
- Villeneuve MY and Casanova C.** On the use of isoflurane versus halothane in the study of visual response properties of single cells in the primary visual cortex. *J Neurosci Methods* 129: 19–31, 2003.